Electronic Supplementary Information

Synthesis, Photophysical Properties, and Excited State Dynamics of Platinum Complex of Tetracene Imide Disulfide (TIDS)

Takafumi Nakagawa,[a] Tsuyoshi Suzuki,[a] Matthias König,[b] Dirk M. Guldi,*[b] and Yutaka Matsuo*[a]

[a] *Department of Chemistry, School of Science, The University of Tokyo*
7-3-1 Hongo, Bunkyo-ku, Tokyo 113-0033, Japan

[b] *Department of Chemistry and Pharmacy and Interdisciplinary Center for Molecular Materials (ICMM), Friedrich-Alexander-Universität Erlangen-Nürnberg,*
Egerlandstrasse 3, Erlangen 91058, Germany

E-mail: dirk.guldi@fau.de; matsuo@chem.s.u-tokyo.ac.jp

– Table of Contents –

1. Experimental S2

2. Structural Feature and Cyclic Voltammogram for Pt(HexylTIDS)(PPh$_3$)$_2$ S4

3. Photophysical Data for HexylTIDS and Pt(HexylTIDS)(PPh$_3$)$_2$ S5

4. NMR spectra for Pt(HexylTIDS)(PPh$_3$)$_2$ S12

1. Experimental

General. All reactions dealing with air or moisture-sensitive compounds were carried out in a dry reaction vessel under argon. Analytical thin-layer chromatography was performed on glass plates coated with 0.25 mm 230–400 mesh silica gel containing a fluorescent indicator (Merck). Flash silica gel column chromatography was performed on silica gel (Wako, Wakogel® C-200). Size exclusion column chromatography was performed on a Japan Analytical Industry LC-9201 (eluent: toluene) with JAIGEL 2H and 3H polystyrene columns. NMR spectra were measured on JEOL ECA-500 and ECX-400 spectrometers and reported in parts per million from tetramethylsilane. High-resolution mass spectra were acquired by atmospheric pressure ionization (APCI) using a time-of-flight mass analyzer on JEOL JMS-T100LC (AccuTOF) spectrometer. UV-vis absorption spectra were recorded on a JASCO V-670 spectrometer.

Materials. Hexyl TIDS was prepared accorrding to our previous report (ref. 8 in the main text). $Pt(PPh_3)_3$ and $Pt(PPh_3)_2(C_2H_4)$ were synthesized through the reported procedures.[S1] The other materials were purchased from Tokyo Kasei Co., Sigma Aldrich Inc. and other commercial suppliers and used after appropriate purification. Solvents were purchased from Kanto Chemical Co., Inc and purified by solvent purification system (GlassContour) equipped with columns of activated alumina and supported copper catalyst (Q-5) prior to use.

Synthesis of Pt(HexylTIDS)(PPh$_3$)$_2$. Method A) A mixture of HexylTIDS (450 mg, 1.02 mmol) and $Pt(PPh_3)_3$ (1.00 g, 1.02 mmol) in THF (30 mL) was stirred at room temperature for 4 h under argon gas atmosphere. Proceeding of the reaction was monitored by ^1H and ^{31}P NMR measurements. To the reaction mixture was added hexane to precipitate the product, which was washed with hexane to obtain Pt(HexylTIDS)$(PPh_3)_2$ as green crystals (820 mg, 70% isolated yield).

Method B) A mixture of HexylTIDS (44.4 mg, 0.100 mmol) and $Pt(PPh_3)_2(C_2H_4)$ (100.1 mg, 0.134 mmol) in THF (3.0 mL) was stirred at room temperature for 1 h under argon gas atmosphere. Proceeding of the reaction was monitored by ^1H and ^{31}P NMR measurements. To the reaction mixture was added hexane to precipitate the product, which was washed with hexane to obtain Pt(HexylTIDS)$(PPh_3)_2\cdot$2THF as green crystals (119.8 mg, 92% isolated yield).

^1H NMR (400 MHz, $CDCl_3$): δ = 0.88 (t, *J* = 6.9 Hz, 3H, Me in hexyl), 1.30–1.38 (m, 4H, CH_2 in hexyl), 1.46–1.52 (m, 2H, CH_2 in hexyl), 1.79–1.85 (m, 2H, CH_2 in hexyl), 4.34 (t, *J* = 7.6 Hz, 2H, CH_2 in hexyl), 7.07 (ddd, *J* = 1.4, 6.6, 8.9 Hz, 2H, 2- and

9-tetracene), 7.22 (t, J = 7.6 Hz, 12H, *o*-Ph), 7.37 (t, J = 7.3 Hz, 6H, *p*-Ph), 7.52-7.58 (m, 14H, *m*-Ph overlapping with 3- and 8-tetracene), 8.45 (dd, J = 0.85, 8.9 Hz, 2H, 1- and 10-tetracene), and 9.83 (dd, J = 0.60, 8.4 Hz, 2H, 4- and 7-tetracene). $^{13}C\{^1H\}$ NMR (100 MHz, $CDCl_3$): δ = 14.1, 22.7, 27.2, 28.2, 31.8, 40.8, 108.3, 123.7, 126.4, 128.1, 128.5, 128.8, 129.1, 129.5, 130.4, 131.0, 132.3, 134.0, 135.0, 153.0, and 164.5. $^{31}P\{^1H\}$ NMR (161 MHz, $CDCl_3$): δ = 21.1 (s, with ^{195}Pt satellites, $J_{Pt\text{-}P}$ = 3040 Hz). IR (ZnSe): ν(C=O)/cm^{-1} 1646 and 1605 (s). HR-MS (APCI$^+$): Calcd. for $C_{62}H_{52}NO_2P_2S_2Pt$ $(M+H)^+$ = 1163.2567, found 1163.2616.

X-ray crystallographic analysis. X-ray crystallographic analysis was performed using a RIGAKU R-AXIS RAPID II (imaging plate detector) with monochromic CuKα (λ = 1.5406 Å) radiation. The positional and thermal parameters were refined by a full-matrix least-squares method using the SHELXL97 program on the Yadokari-software.

Electrochemical Studies. Cyclic voltammetry (CV) was performed using HOKUTO DENKO HZ-5000 voltammetric analyzer. All CV measurements were carried out in a one-compartment cell under argon gas, equipped with a glassy-carbon working electrode, a platinum wire counter electrode, and an Ag/Ag$^+$ reference electrode. The supporting electrolyte was a 0.1 mol/L dichloromethane solution of tetrabutylammonium hexafluorophosphate ($TBAPF_6$). Spectroelectrochemical oxidation was carried out with a setup containing a Varian Cary 5000 UV/vis-NIR spectrometer, a HEKA elektroniks PG 284 potentiostat, and a home-made cell with a three-electrode configuration. As working electrode, a light-transparent platinum gauze was used, whereas a platinum plate and a Ag wire served as counter electrode and reference electrode, respectively. All spectroelectrochemical measurements were done in argon-saturated dichloromethane containing 0.2 M TBAPF6 as supporting electrolyte.

Photophysical studies. All solvents used were spectroscopic grade and were purchased from Sigma-Aldrich. UV/vis spectra were recorded with a Perkin Elmer Lambda 2 instrument. For emission, a FluoroMax 3 fluorometer by HORIBA JobinYvon was used to detect in the visible region (< 800 nm), whereas a HORIBA JobinYvon Fluorolog instrument was applied to detect emission in the NIR region. All UV/vis absorption and emission studies were carried out in argon saturated solutions in a 10 x 10 mm quartz cell. For singlet oxygen detection, the samples were instead purged with oxygen. Femtosecond transient absorption studies were performed in argon-saturated solutions with 387 nm, 656 nm and 670 nm excitation laser pulses (1 kHz, 150 fs pulse width) from an amplified Ti:Sapphire laser system (Clark-MXR Inc.) with a laser energy of 200 nJ. Nanosecond laser flash photolysis experiments were carried out with argon or oxygen purged samples using a 355 nm laser pulse from a Quanta-Ray CDR Nd:Yag system (6 ns pulse width) in a front face excitation geometry.

S1 (a) R. Ugo, F. Cariati and G. La Monica, *Inorg. Synth.*, 1968, **11**, 105. (b) D. M. Blake, D. M. Roundhill, C. Ambridge, S. Dwight and H. C. Clark, *Inorg. Synth.,* 1978, **18**, 120.

2. Structural Feature and Cyclic Voltammogram for Pt(HexylTIDS)$(PPh_3)_2$

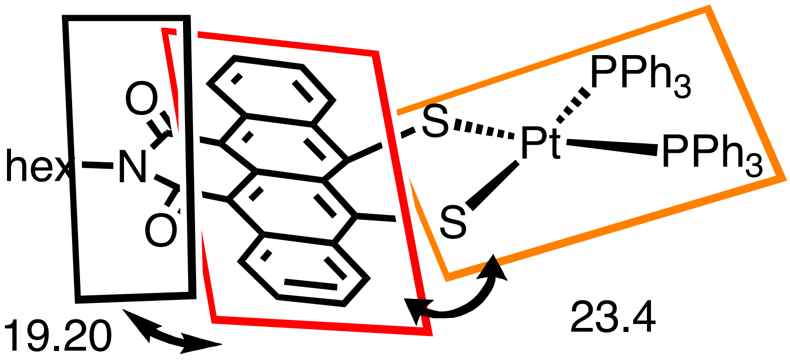

Figure S1. Distorted structure of Pt(HexylTIDS)$(PPh_3)_2$.

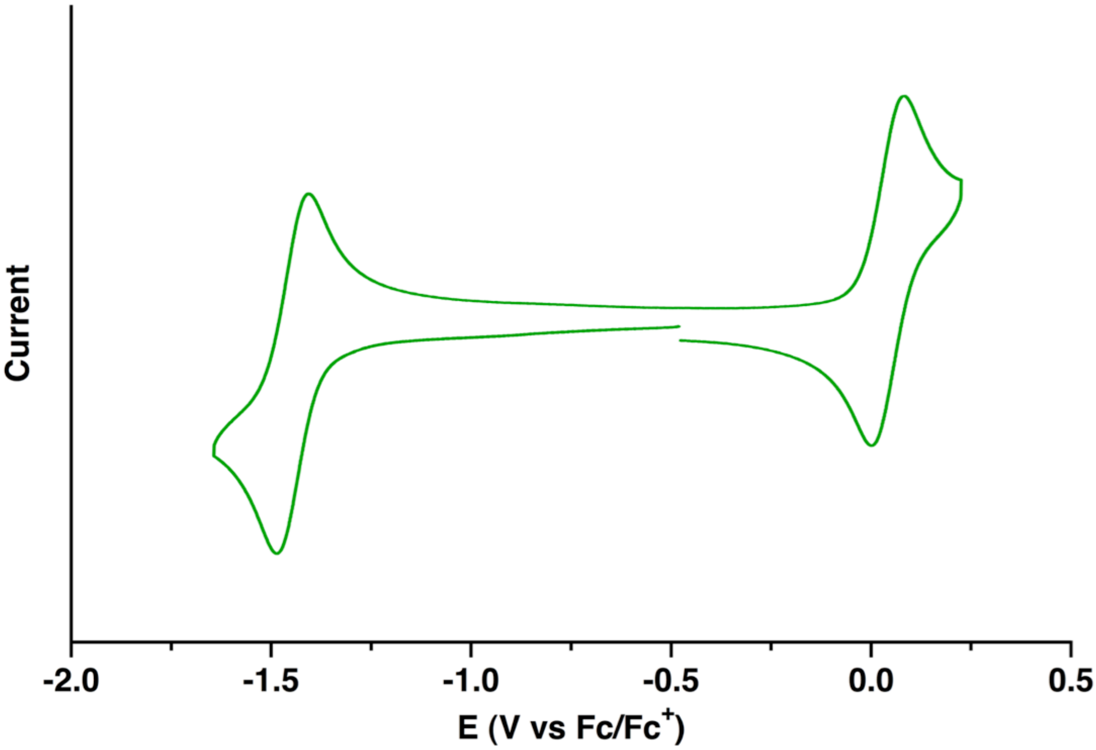

Figure S2. Cyclic voltammogram of Pt(HexylTIDS)$(PPh_3)_2$.

3. Photophysical Data for HexylTIDS and Pt(HexylTIDS)(PPh_3)$_2$

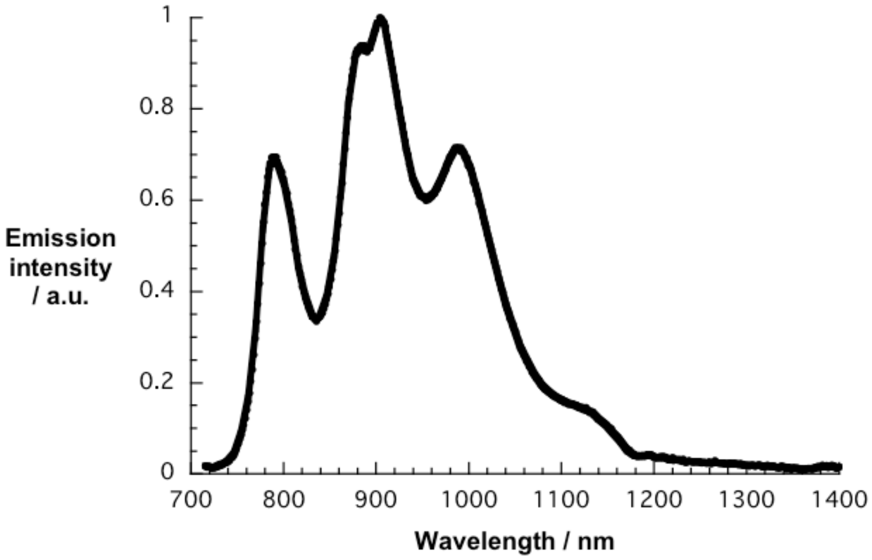

Figure S3. Steady-state emission spectrum (λ_{ex} = 692 nm) of HexylTIDS in argon-saturated THF at room temperature.

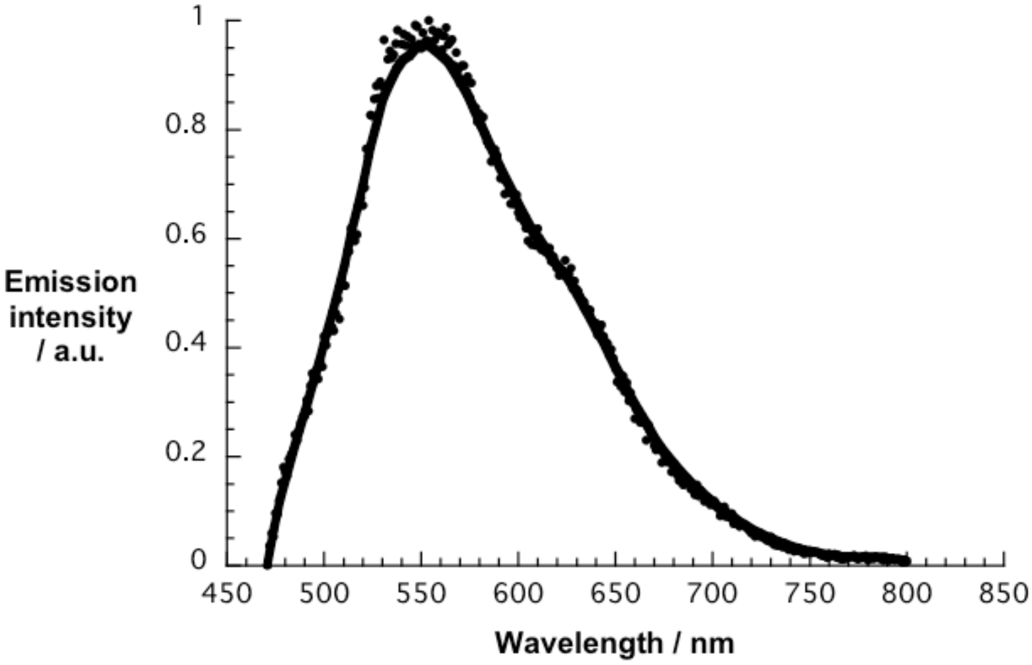

Figure S4. Steady-state emission spectrum (λ_{ex} = 387 nm) showing the S_2 fluorescence of Pt(HexylTIDS)(PPh_3)$_2$ in argon-saturated THF at room temperature.

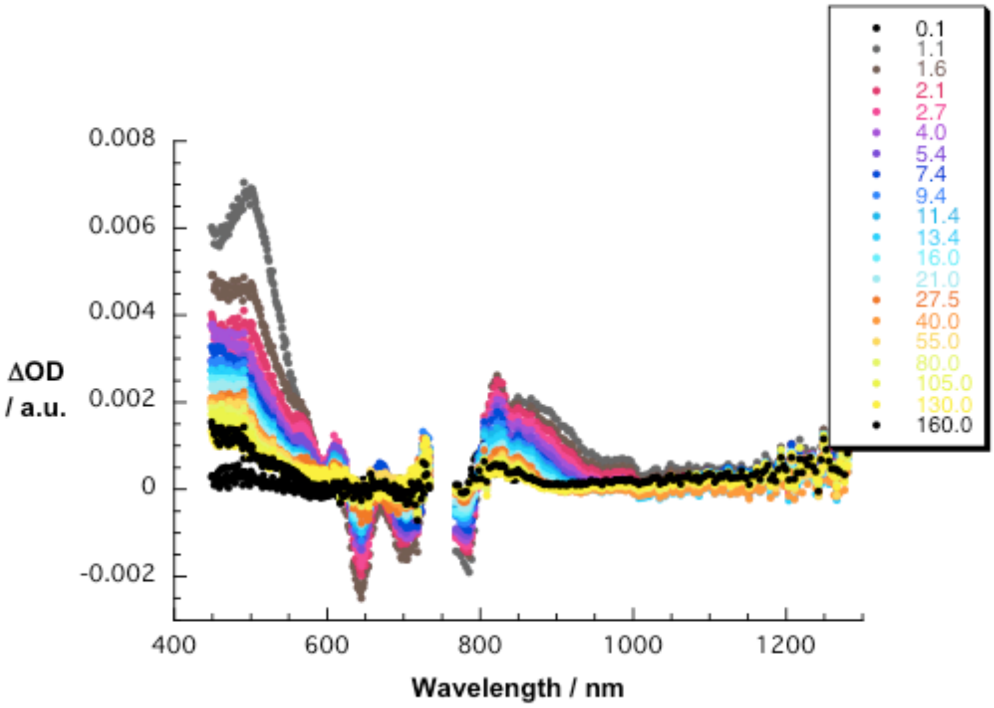

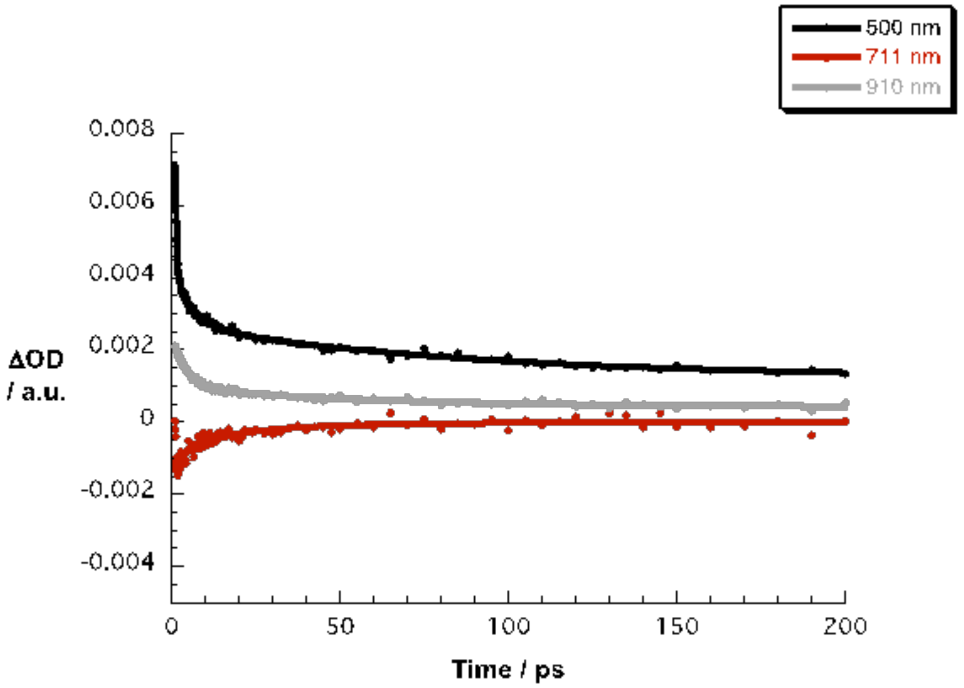

Figure S5. Upper part – differential absorption spectra of HexylTIDS obtained upon femtosecond flash photolysis (λ_{ex} = 387 nm) in argon-saturated THF with several time delays between 0.1 and 160 ps. OD at the excitation wavelength was 0.22. Lower part – time absorption profiles of the spectra shown above at 500, 711, and 910 nm.

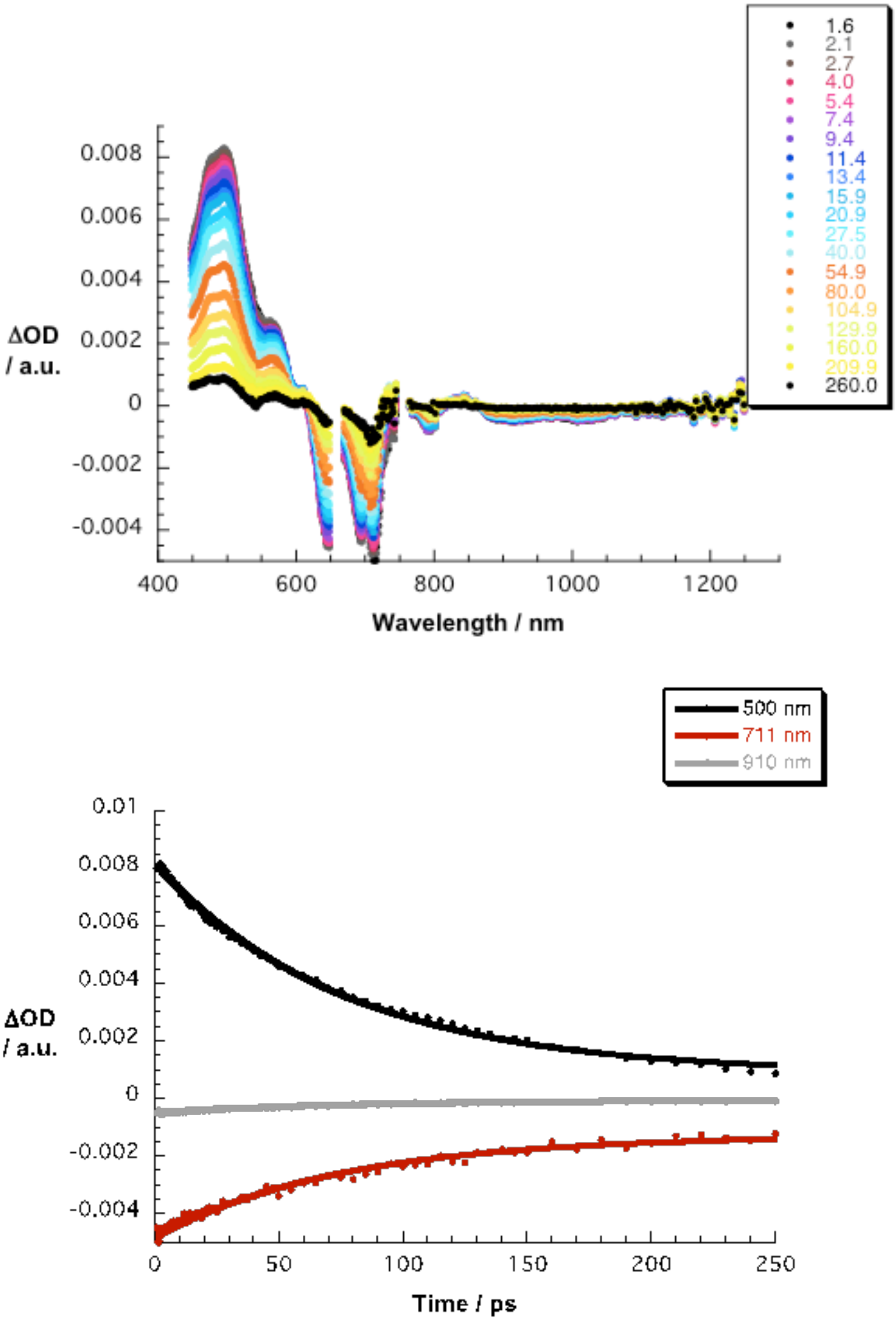

Figure S6. Upper part – differential absorption spectra of HexylTIDS obtained upon femtosecond flash photolysis (λ_{ex} = 656 nm) in argon-saturated THF with several time delays between 1.6 and 260 ps. OD at the excitation wavelength was 0.22. Lower part – time absorption profiles of the spectra shown above at 500, 711, and 910 nm.

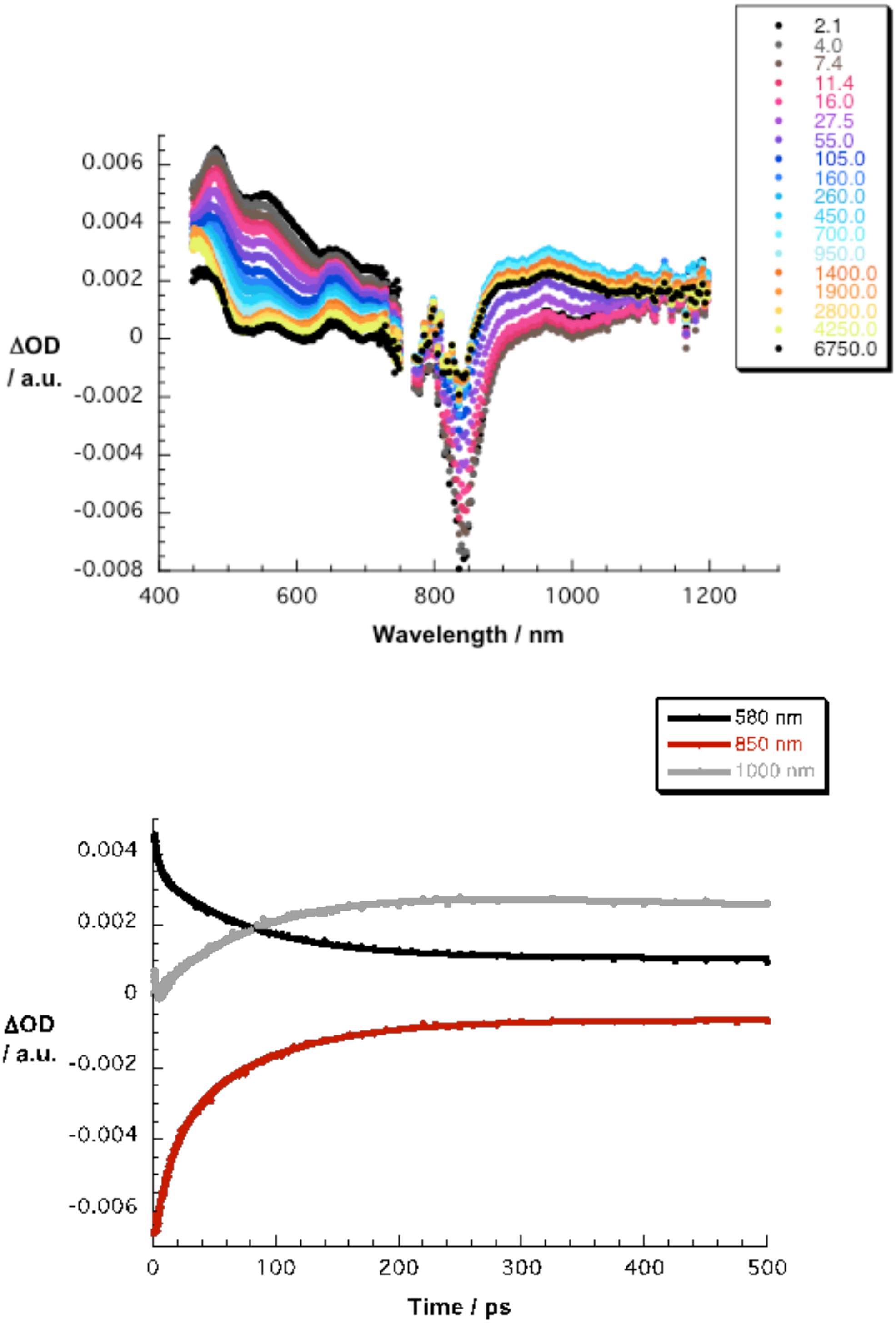

Figure S7. Upper part – differential absorption spectra of Pt(HexylTIDS)$(PPh_3)_2$ obtained upon femtosecond flash photolysis (λ_{ex} = 387 nm) in argon-saturated THF with several time delays between 2.1 and 6750 ps. OD at the excitation wavelength was 0.26. Lower part – time absorption profiles of the spectra shown above at 580, 850, and 1000 nm.

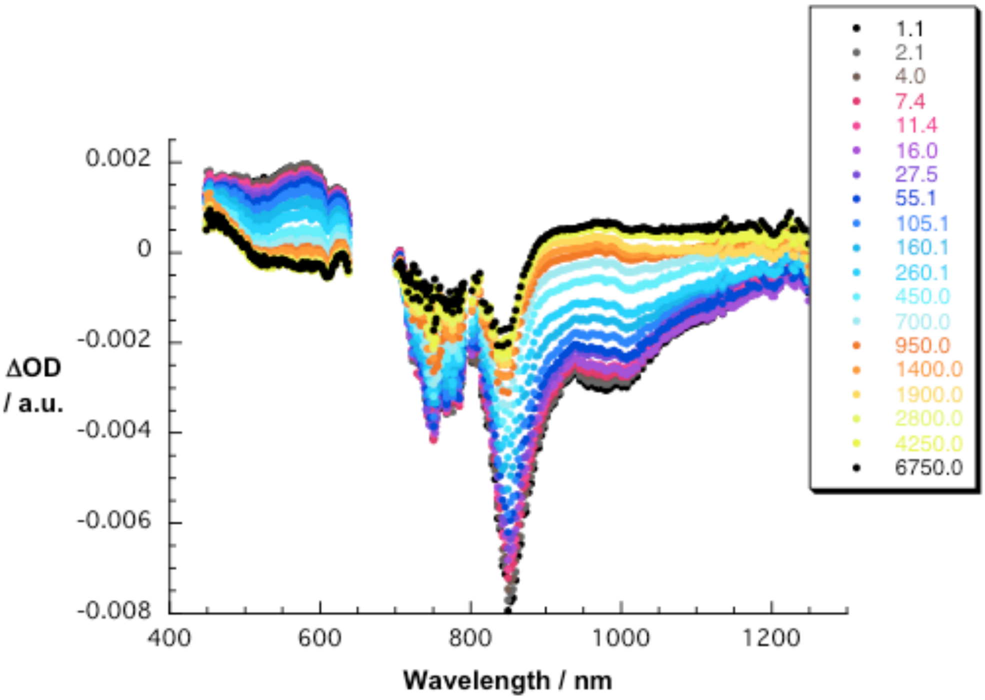

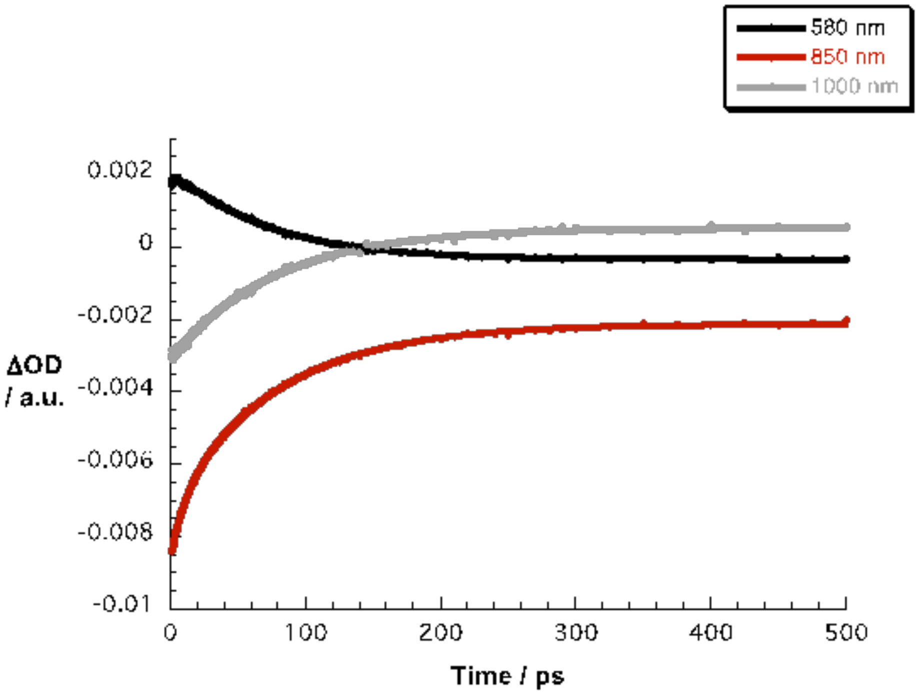

Figure S8. Upper part – differential absorption spectra of Pt(HexylTIDS)$(PPh_3)_2$ obtained upon femtosecond flash photolysis (λ_{ex} = 670 nm) in argon-saturated THF with several time delays between 1.1 and 6750 ps. OD at the excitation wavelength was 0.18. Lower part – time absorption profiles of the spectra shown above at 580, 850, and 1000 nm.

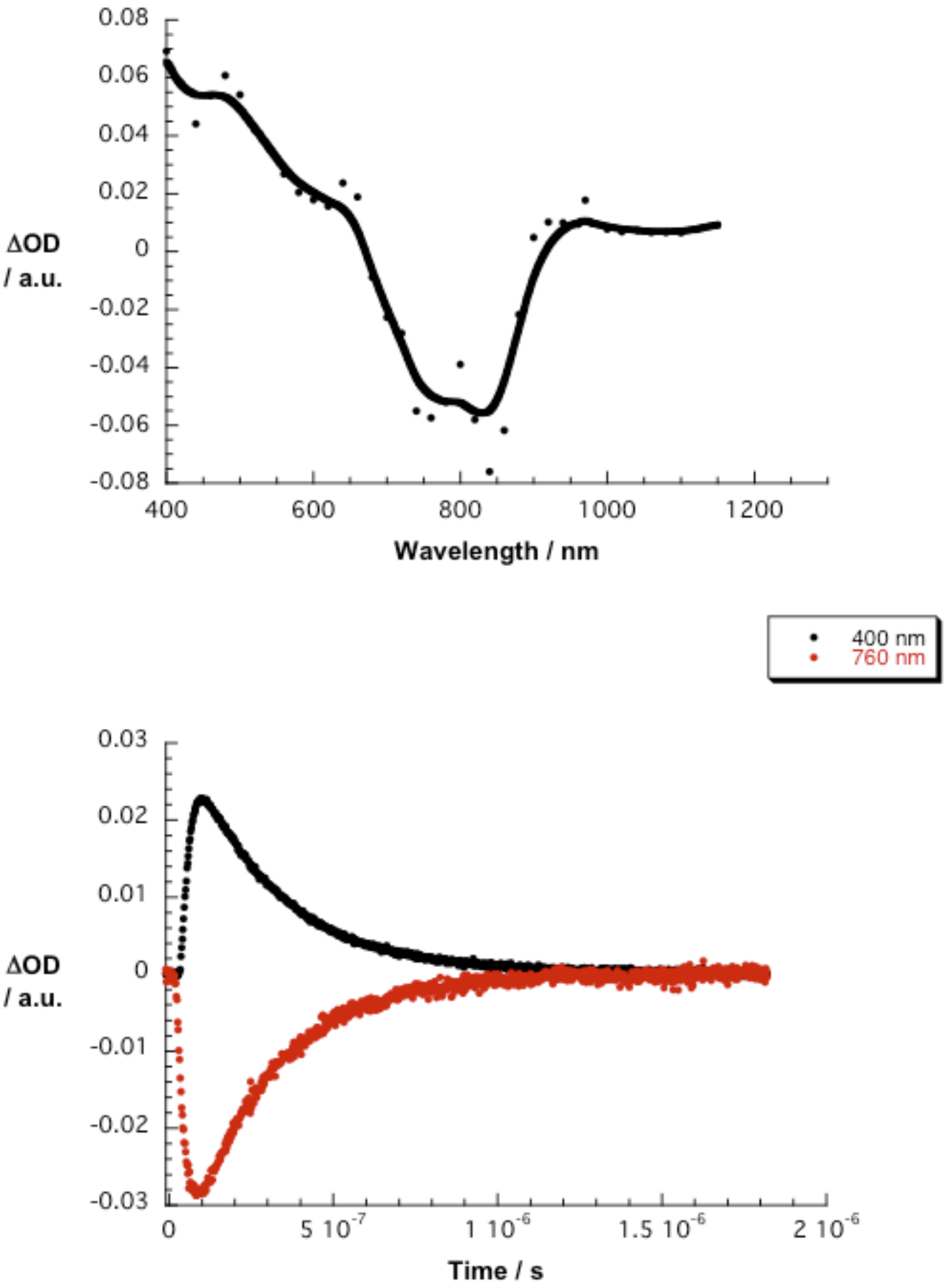

Figure S9. Upper part – differential absorption spectrum of Pt(HexylTIDS)$(PPh_3)_2$ obtained upon nanosecond flash photolysis (λ_{ex} = 355 nm) in argon-saturated THF with a time delay of 110 ns. Lower part – time absorption profiles of the spectra shown above at 400 and 760 nm.

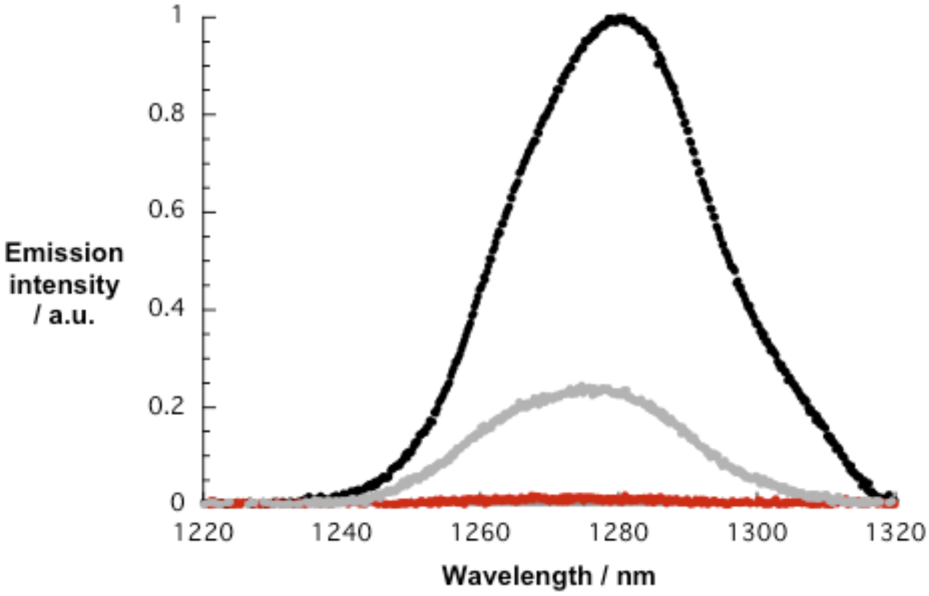

Figure S10. Singlet oxygen phosphorescence spectra (λ_{ex} = 692 nm) of HexylTIDS (red spectrum), Pt(HexylTIDS)(PPh$_3$)$_2$ (grey spectrum) and a zinc phthalocyanine reference (black spectrum) in oxygen-saturated thf at room temperature. OD at the excitation wavelength was 0.1 for all samples.

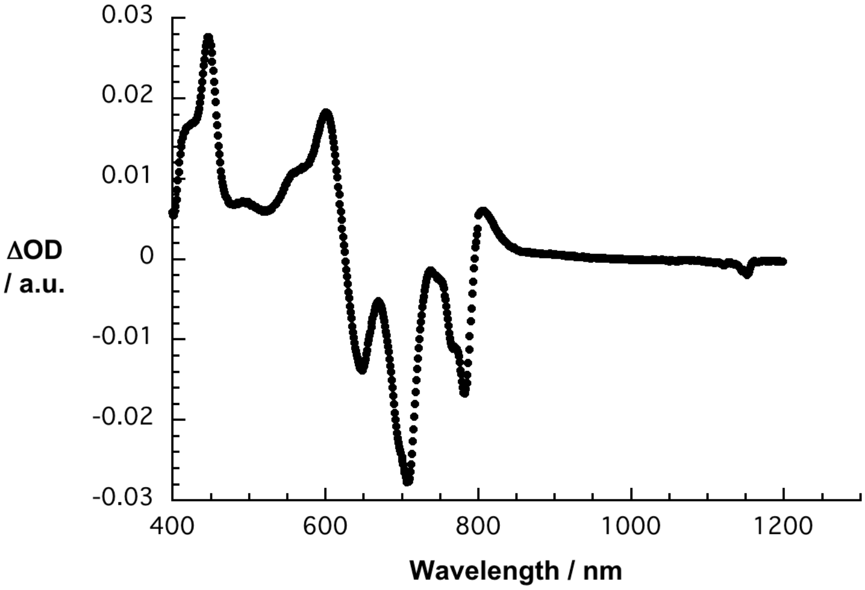

Figure S11. Spectroelectrochemical oxidation of HexylTIDS at +0.8 V *vs* Fc in dichloromethane containing 0.2 M tetrabutylammonium hexafluorophosphate as supporting electrolyte.

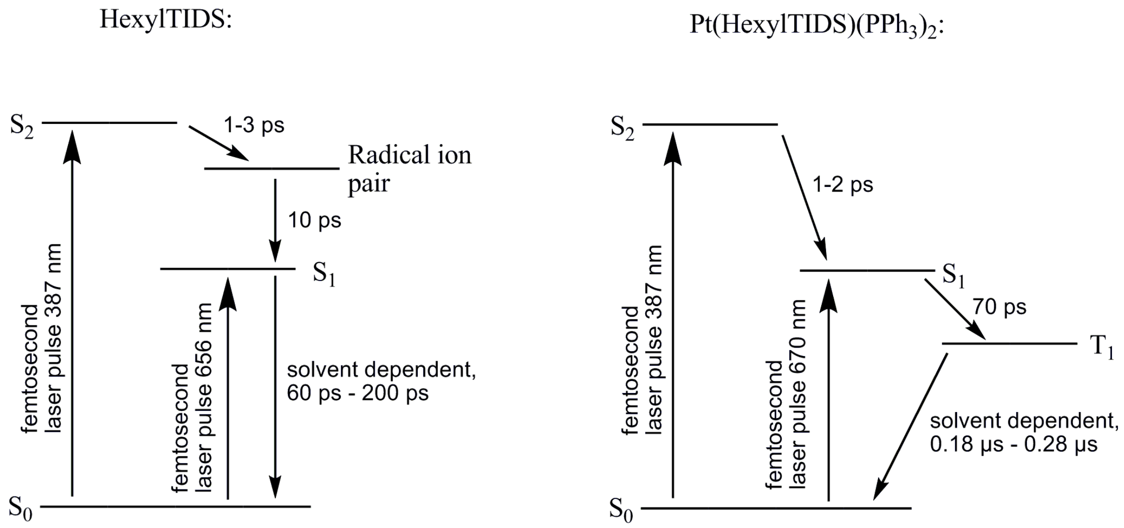

Figure S12. Energy diagram illustrating the pathways commencing with the photoexcitation of HexylTIDS (left) and Pt(HexylTIDS)(PPh$_3$)$_2$ (right).

4. NMR spectra for Pt(HexylTIDS)(PPh$_3$)$_2$

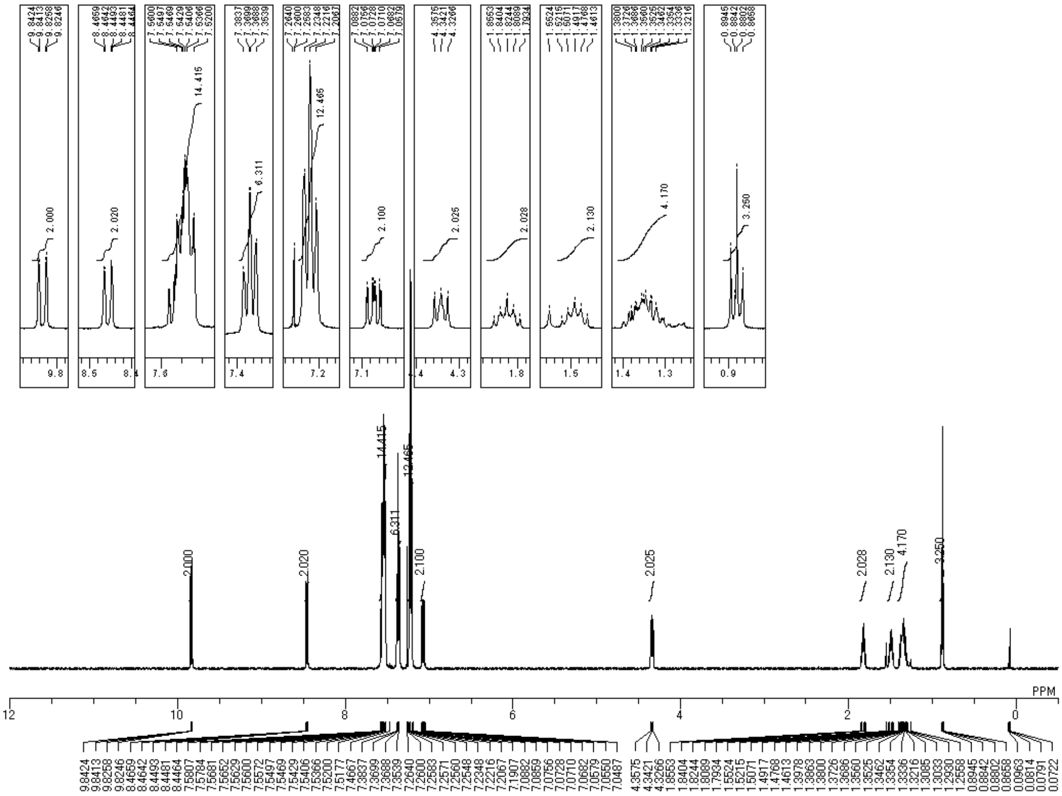

Figure S13. ^{1}H NMR chart for Pt(HexylTIDS)(PPh$_3$)$_2$.

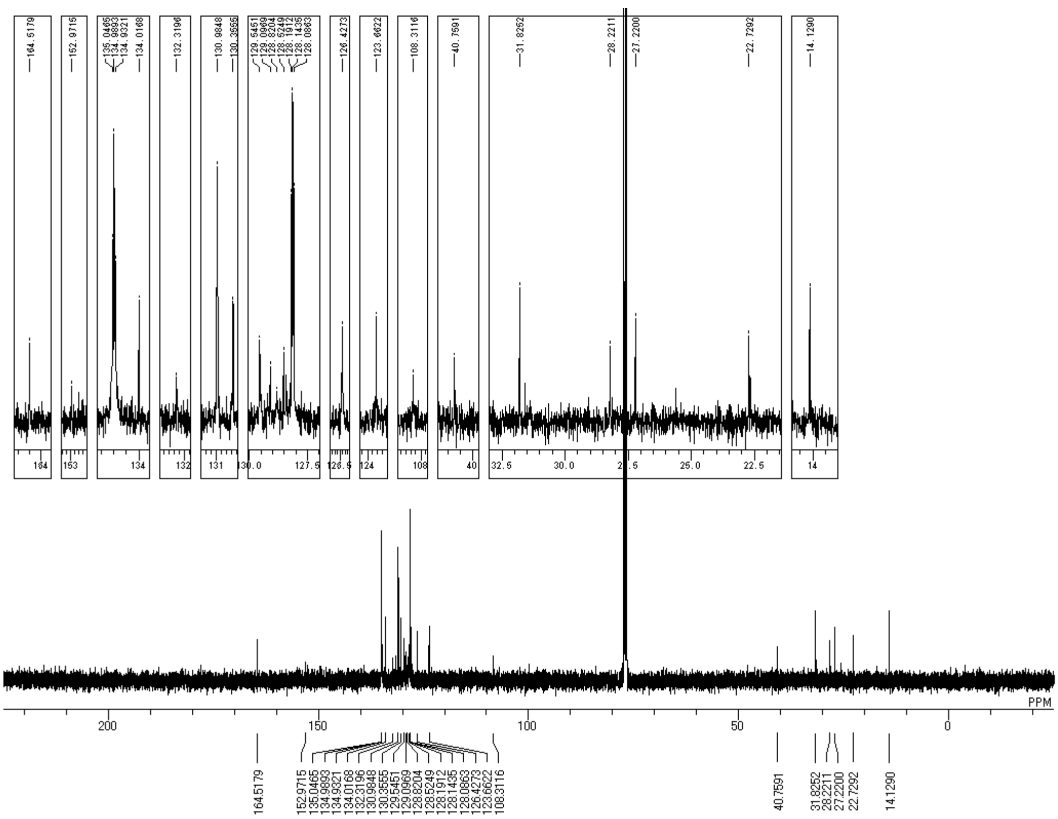

Figure S14. ^{13}C NMR chart for Pt(HexylTIDS)(PPh$_3$)$_2$.

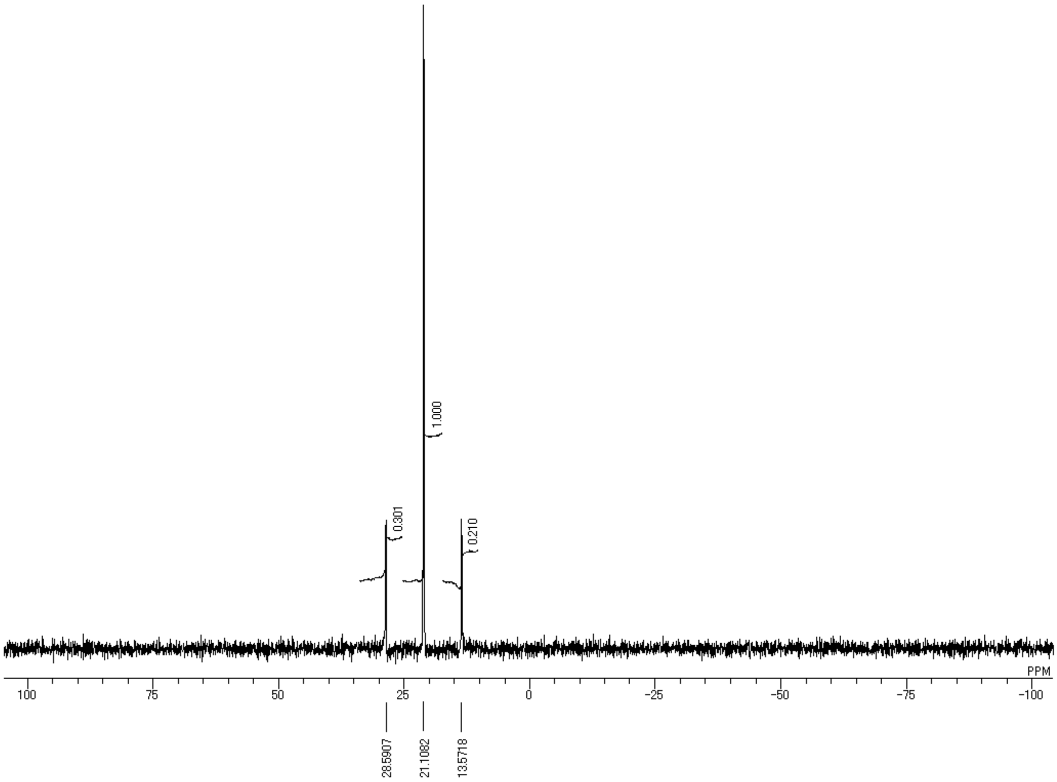

Figure S15. ^{31}P NMR chart for Pt(HexylTIDS)(PPh_3)$_2$.